

Developing an Air Separation Reactor

Design from the Carrier to the Reactor



Jonathan W. Lekse

Pittsburgh Coal Conference, September 10, 2020

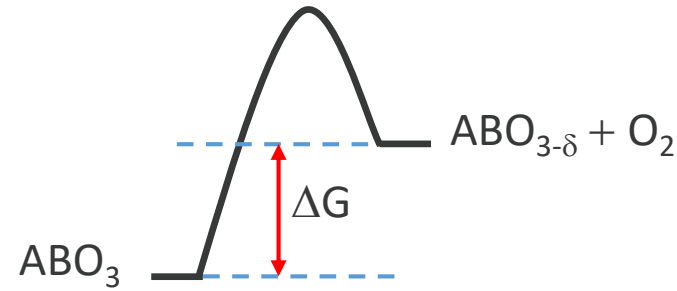
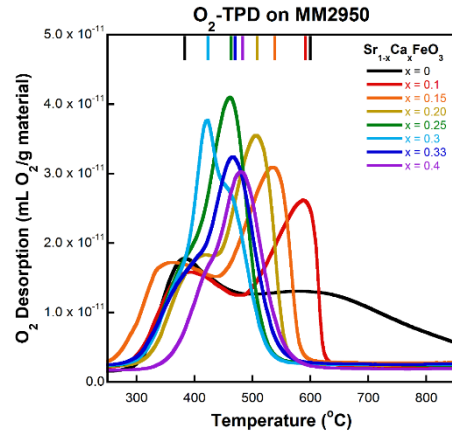


Solutions for Today | Options for Tomorrow

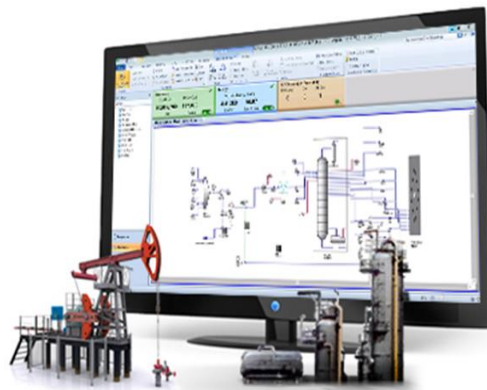
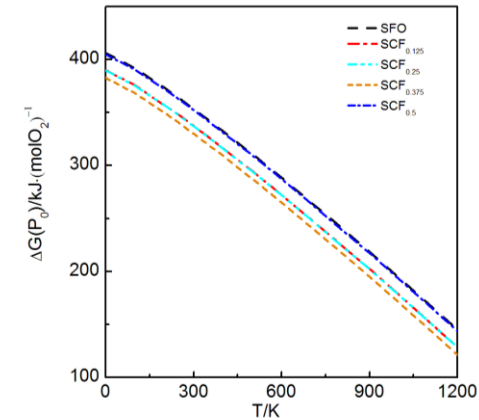
Background

Project Goal: Linking Atomic and Process Scales

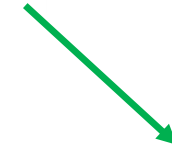
Laboratory Experiments and Atomistic Modelling



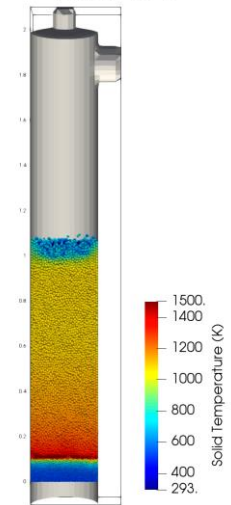
Ellingham Diagrams



Process Models



Time: 724s

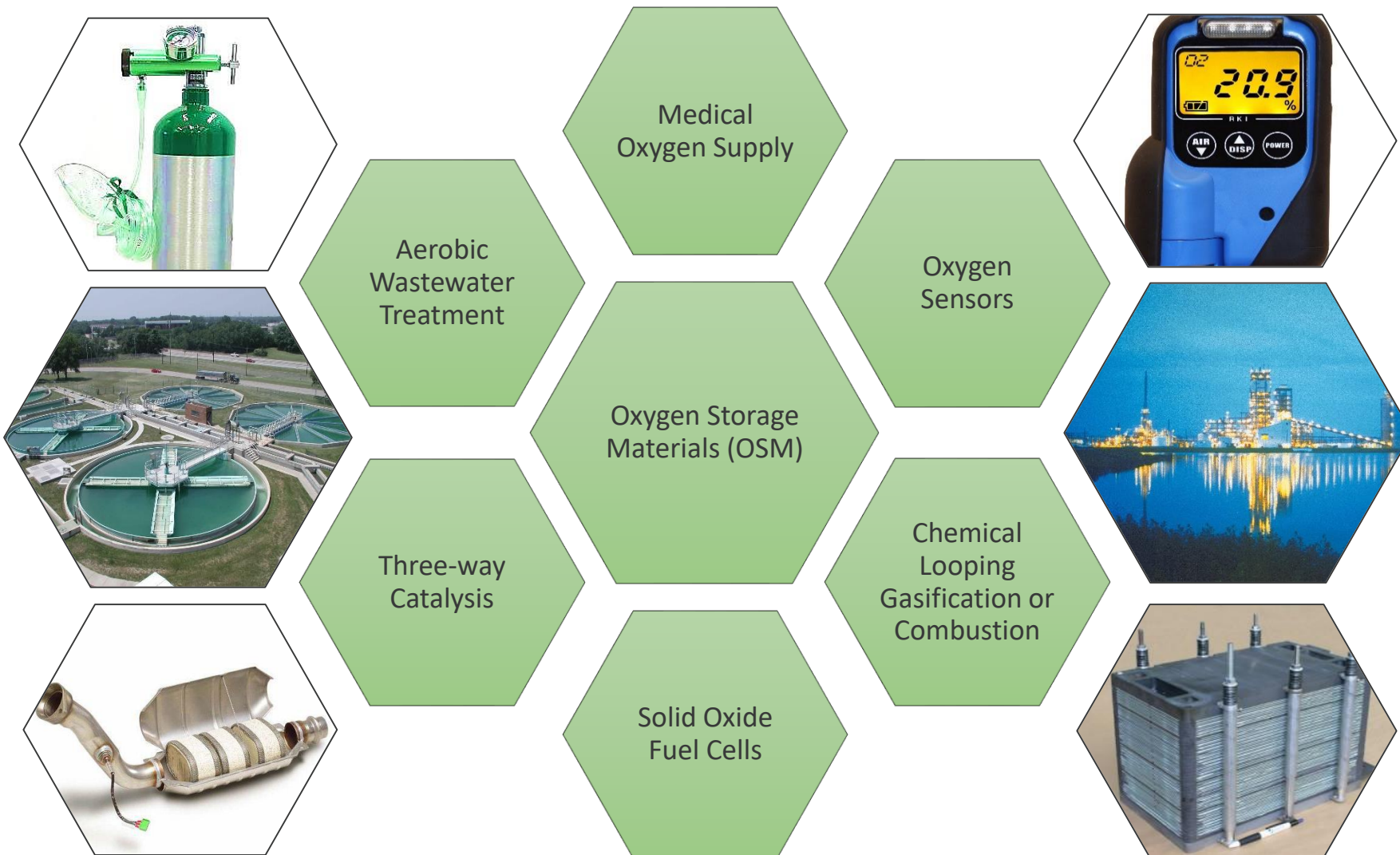


Reactor Design and CFD M



Background

Current and potential uses for Oxygen Storage Materials

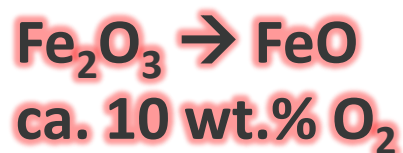


Background

Current Regenerable Oxygen Carriers

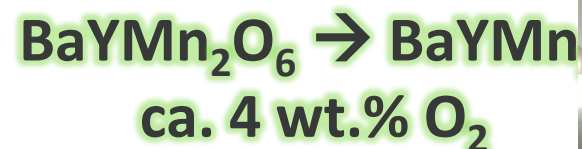
Stoichiometric Oxides

- Materials include: Fe_2O_3 , Co_3O_4 , $\text{M}_x\text{Fe}_2\text{O}_4$, $\text{M}_{2-x}\text{M}'_x\text{O}_3$ etc.
- Structural oxygen release/uptake
 - Large oxygen storage potential
 - High temperatures required
 - Extensive structural rearrangement necessary



Non-stoichiometric Oxides

- Materials include: $\text{BaYMn}_2\text{O}_{5+\delta}$, $\text{YBa}(\text{Co}_{1-x}\text{Ga}_x)_4\text{O}_{7+\delta}$, $\text{Ca}_2\text{AlMnO}_{5+\delta}$, $\text{Sr}_3\text{Fe}_2\text{O}_{7-\delta}$, etc.
- Interstitial or labile oxygen release/uptake
 - Lower oxygen storage potentials
 - Lower temperatures possible
 - Much less structural rearrangement necessary

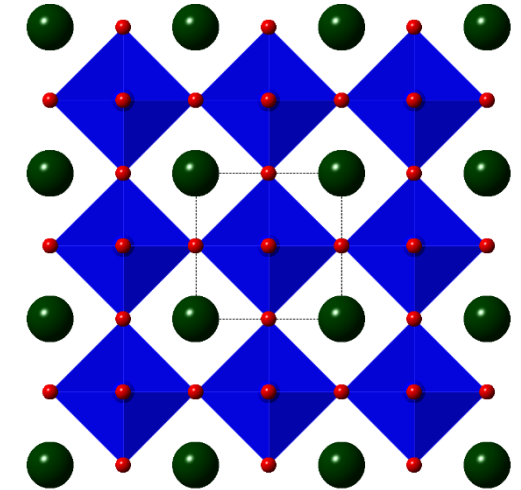


Perovskite Materials

Background

- Perovskites are a well studied type of oxide with the general formula ABO_3
- The first identified Perovskite was $CaTiO_3$
- A-site cation has a dodecahedral coordination
- B-site cation sits in the center of BO_6 octahedra
- “Ideal” structure is cubic though the size of the A-site cation can create distortions

- Applications
 - Chemical looping combustion
 - Potential CLOU candidates, if oxygen is released into the gas phase
 - Pollution remediation
 - NO_x decomposition
 - Replacement of noble metal catalysts in automobiles
 - Syngas production via reforming reactions
 - High Temperature Gas Sensors
 - Solid Oxide Fuel Cells
 - Photovoltaics
- Potentially Interesting Properties
 - Superconductivity
 - Magnetoresistance
 - Ferromagnetism



ABO_3

1 H	2 He																			
3 Li	4 Be	5 B	6 C	7 N	8 O	9 F	10 Ne													
11 Na	12 Mg	13 Al	14 Si	15 P	16 S	17 Cl	18 Ar													
19 K	20 Ca	21 Sc	22 Ti	23 V	24 Cr	25 Mn	26 Fe	27 Co	28 Ni	29 Cu	30 Zn	31 Ga	32 Ge	33 As	34 Se	35 Br	36 Kr			
37 Rb	38 Sr	39 Y	40 Zr	41 Nb	42 Mo	43 Tc	44 Ru	45 Rh	46 Pd	47 Ag	48 Cd	49 In	50 Sn	51 Sb	52 Te	53 I	54 Xe			
55 Cs	56 Ba	57-70 * Lu	71 Hf	72 Ta	73 W	74 Re	75 Os	76 Ir	77 Pt	78 Au	79 Hg	80 Tl	81 Pb	82 Bi	83 Po	84 At	85 Rn	86		
87 Fr	88 Ra	89-102 ** Lr	103 Rf	104 Db	105 Sg	106 Bh	107	108	109	110	111	112	113	114	115	116	117	118	119	120

* Lanthanide series

57 La	58 Ce	59 Pr	60 Nd	61 Pm
89 Ac	90 Th	91 Pa	92 U	93 Np

** Actinide series



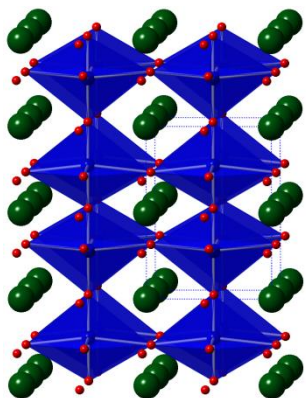
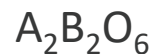
Perovskite Materials

Chemical Substitution

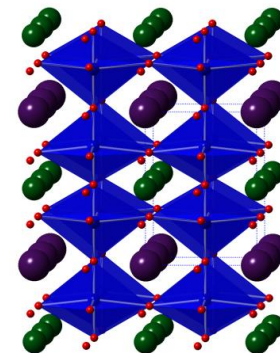
General Perovskite Formula



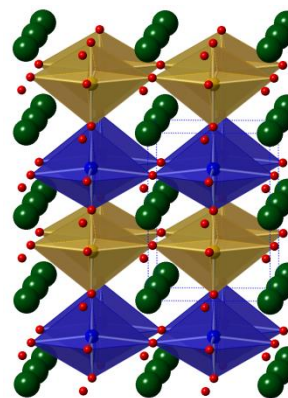
Doubled Perovskite Formula



A-Site Substitution



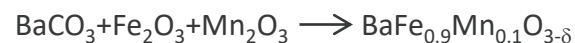
B-Site Substitution



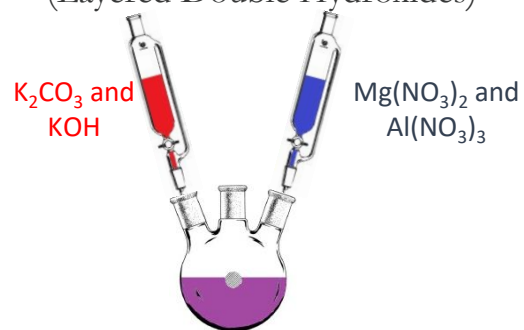
NETL Material Synthesis Capabilities

Perovskite Synthesis

High-Temperature Solid-State
(Bulk Delafossites and Perovskites)

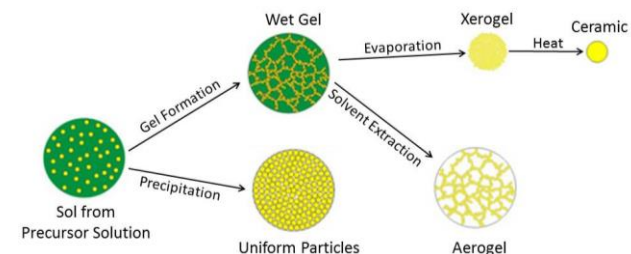


Precipitation/Co-precipitation
(Layered Double Hydroxides)

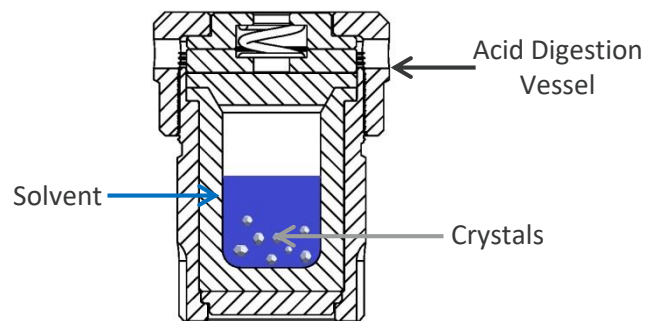


LDH Product

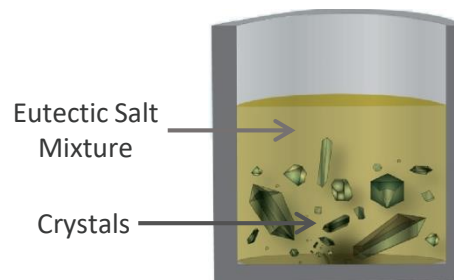
Sol-Gel Methods
(Complex Metal Oxide Nanoparticles)



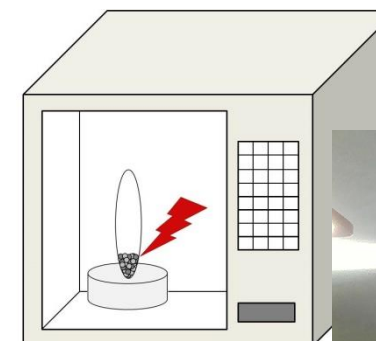
Solvothermal
(Single Crystal Growth)



Salt Flux
(Single Crystal Growth)



Solid State Microwave
(Bulk Chalcogenides)

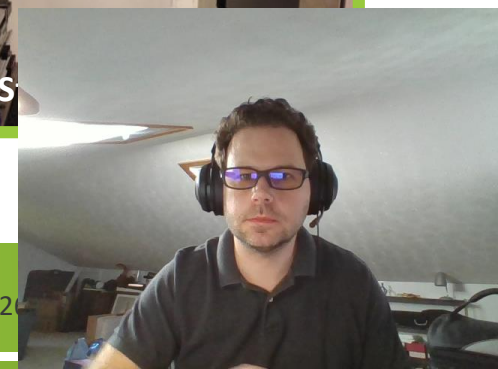
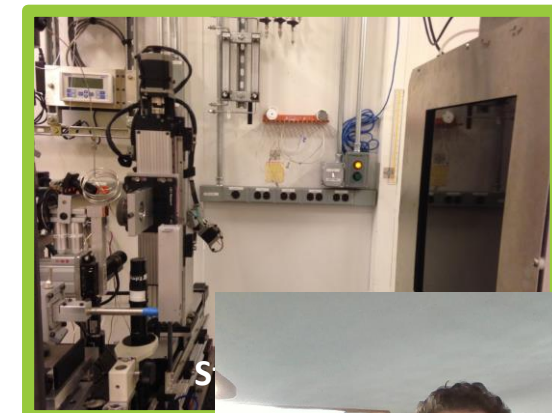
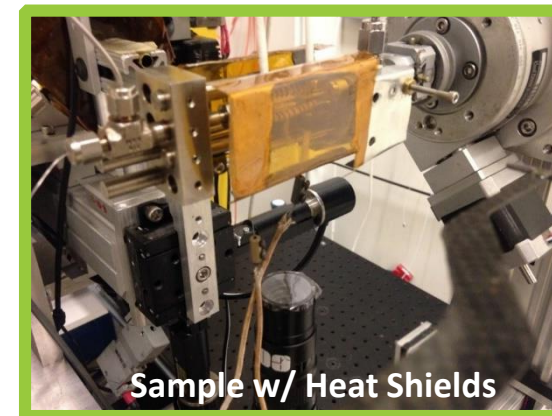
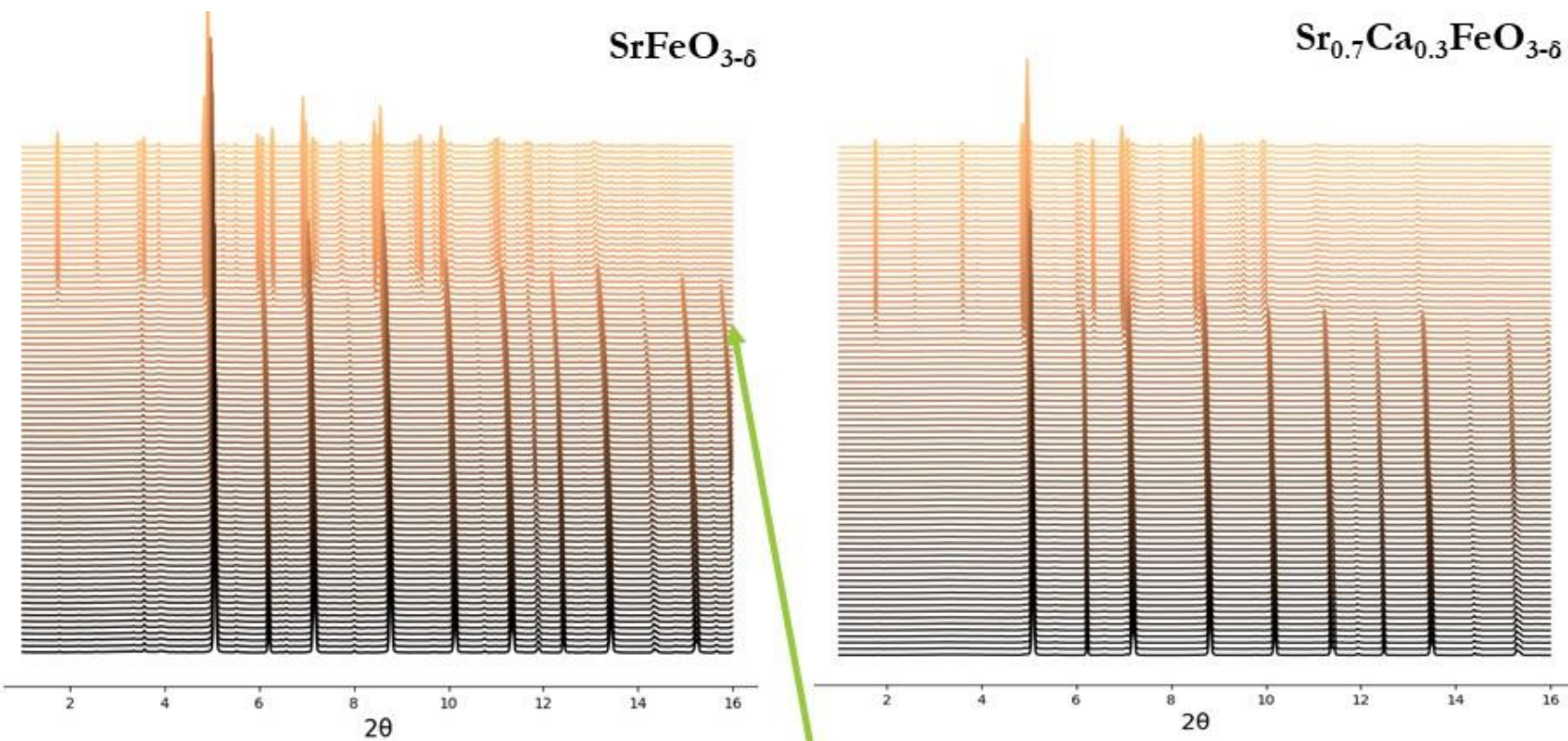


Perovskite Characterization

High-resolution, rapid collection synchrotron powder *in situ* XRD

- **Time-resolved *in situ* XRD**

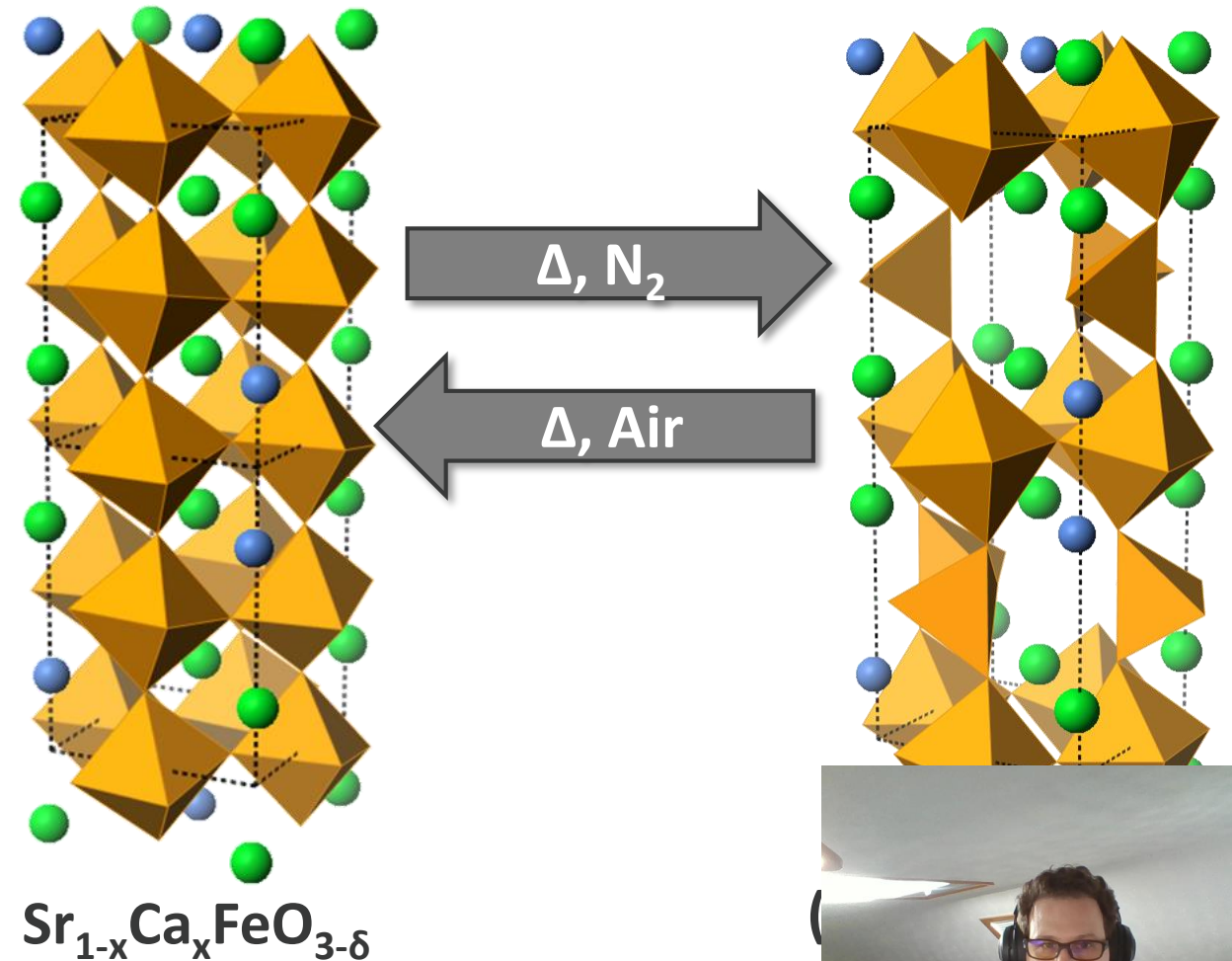
- Determine structural changes in relation to oxygen release
- Synchrotron source (APS 17-BM) - high-energy, rapid acquisition



Perovskite Characterization

Structure Changes

- **Minor conversion between structure-types**
 - Tilt in half of FeO_6 -octahedra
 - Removal of oxygen creating layer of FeO_4 tetrahedra from other half of FeO_6 -octahedra
- **More Ca^{2+} substitution – greater stability as brownmillerite structure**



Perovskite Characterization

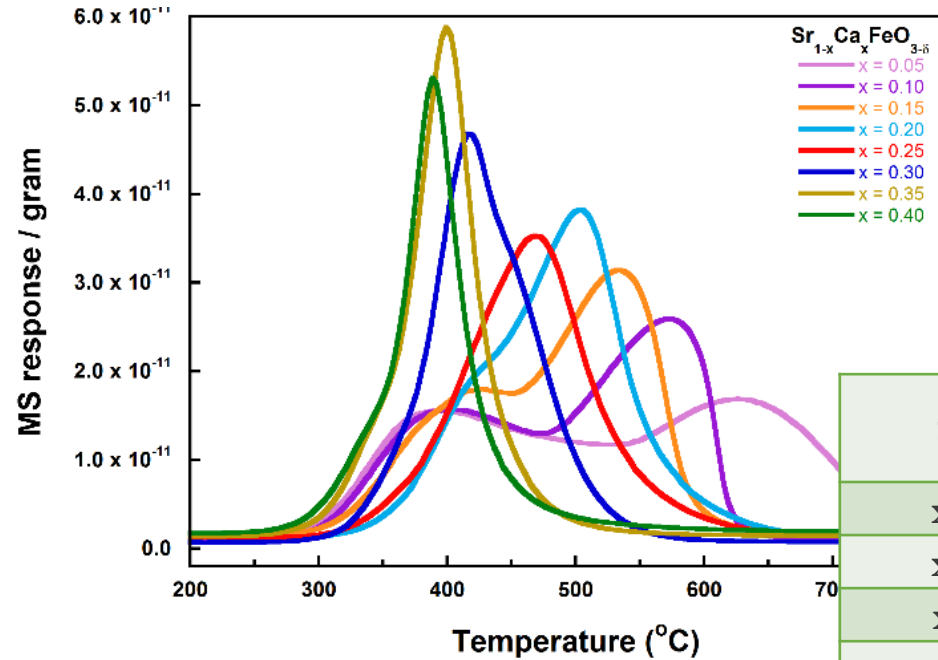
TPD: Determination of maximum O₂ storage capacities and desorption temperatures

- **Experiment:**

- Systematic priming at 850°C in air flow for O₂ uptake for 1 hour
- Cool to RT
- 10 deg/min ramp to 1050°C in He flow and monitor O₂ release

- **Findings:**

- As x increases, T_{des, max} decreases
- As x increases, max O₂ release decreases
- As x increases, α & β oxygen desorption distinctions merge



Sample	Volume O ₂ (mL/g)
x = 0.00	17.134
x = 0.05	16.282
x = 0.10	16.264
x = 0.15	15.292
x = 0.20	15.678
x	
x	
x	
x	



Perovskite Characterization

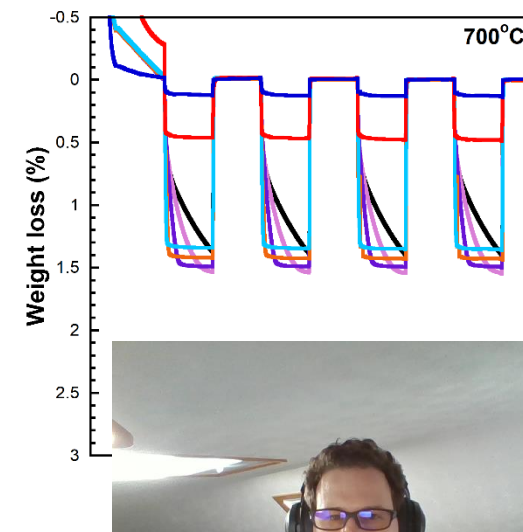
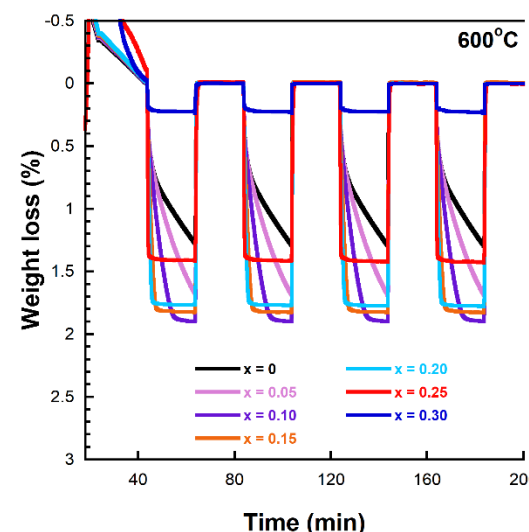
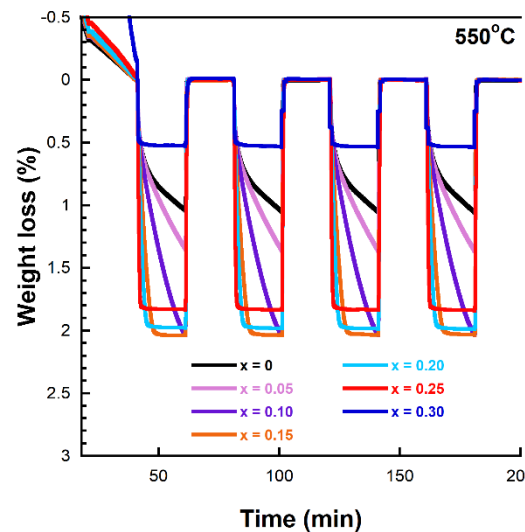
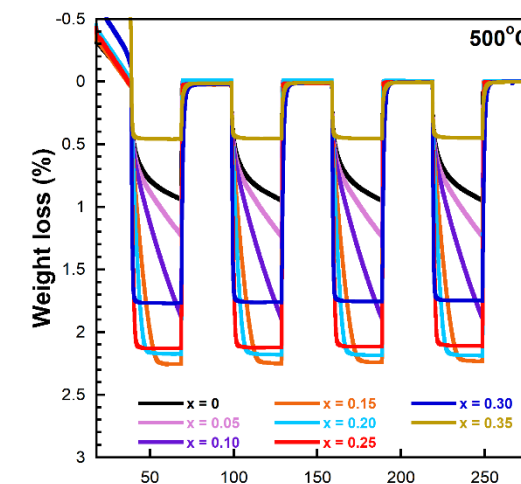
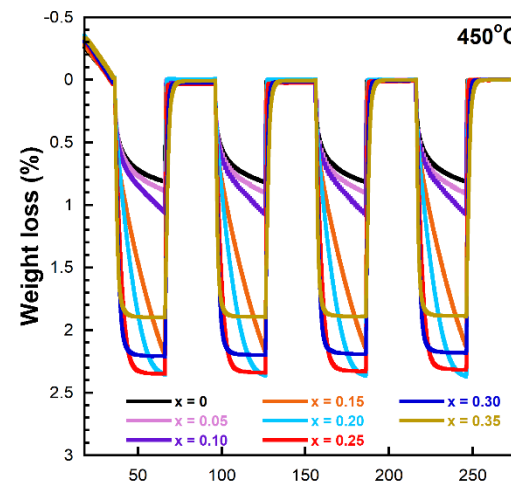
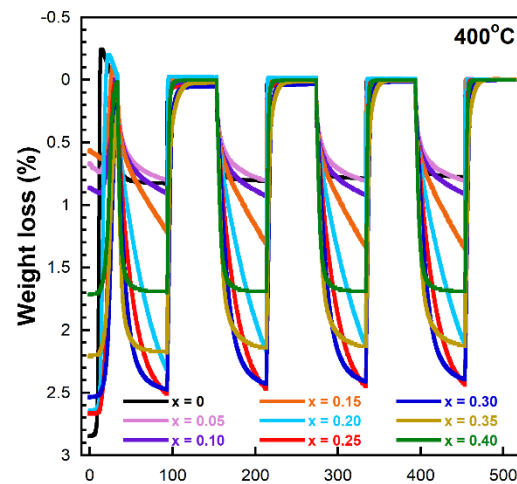
TGA: All samples show cyclable O₂ uptake and release

- **Samples demonstrate durability and cyclability**

- 4 uptake/release cycles
 - Shorter cycle timeframe used for higher temperatures
 - Gas flow (75 sccm)
- Samples aged 6+ mo. in air

- **Findings:**

- As x increases, max O₂ capacity decreases (agrees with O₂-TPD)
- As x increases, max uptake temperature increases
- As x increases, rate of O₂ release at 800°C increases
- If $x \geq 0.30$, sharp decrease in oxygen storage at 450-500°C exists
 - $x = 0.20$, less abrupt at 550-700°C



Perovskite Characterization

TGA: Oxygen storage capacities and time to reach 90% released

- As temperature increases, max OSC decreases
 - Instability of oxidized species under air flow
 - Ex: $x = 0.30$ at 550°C
 $0.54 \text{ wt}\% \text{ O}_2$

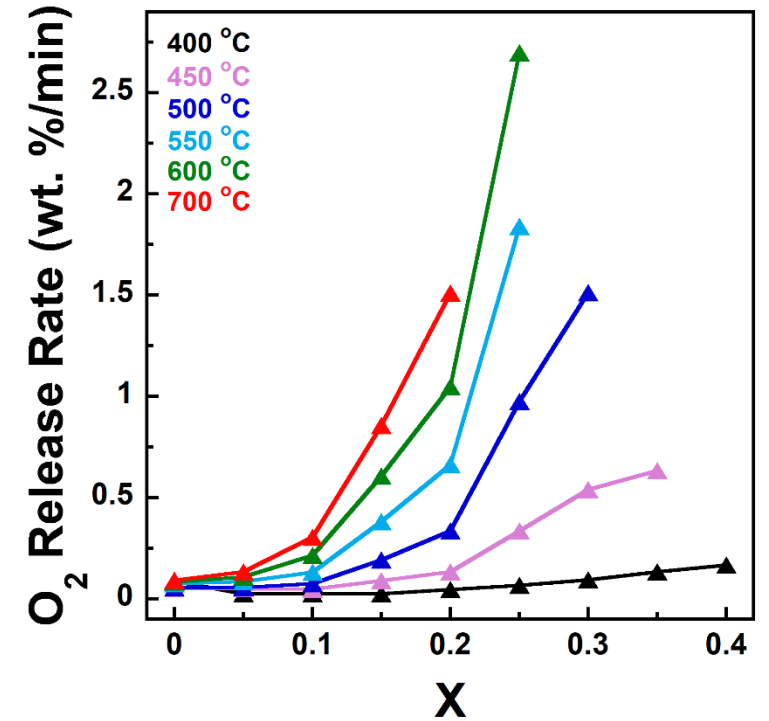
OSC in wt%

		Temperature ($^\circ\text{C}$)					
		400	450	500	550	600	700
Ca ²⁺ ratio (x)	0.00	0.84	0.82	0.95	1.06	1.30	1.40
	0.05	0.81	0.91	1.19	1.37	1.69	1.55
	0.10	0.93	1.08	1.91	2.04	1.90	1.50
	0.15	1.35	2.17	2.26	2.04	1.83	1.44
	0.20	2.10	2.37	2.19	1.99	1.78	1.36
	0.25	2.41	2.35	2.13	1.84	1.43	0.49
	0.30	2.41	2.21	1.77	0.54	0.24	0.14
	0.35	2.13	1.90	0.46			
	0.40	1.72					

- Rates increase as x and temperature increase
 - Disparities due to very low OSCs
 - Only SrFeO_3 stays constant

Time (min) to 90% release

		Temperature ($^\circ\text{C}$)					
		400	450	500	550	600	700
Ca ²⁺ ratio	0.00	9.56	16.53	17.38	13.93	15.58	15.15
	0.05	31.77	18.33	20.70	16.03	15.65	11.67
	0.10	36.03	22.08	25.08	15.47	8.85	4.93
	0.15	51.35	24.22	11.83	5.35	3.02	1.68
	0.20	45.17	17.85	6.53	3.00	1.70	0.90
	0.25	36.13	7.00	2.18	1.00	0.53	1.05
	0.30	25.83	4.10	1.17	0.70	4.72	17.32
	0.35	16.03	3.00	1.07			
	0.40	10.30					



Plot estimates the speed of oxygen release:

$$rate = \frac{dO_2}{dt}$$

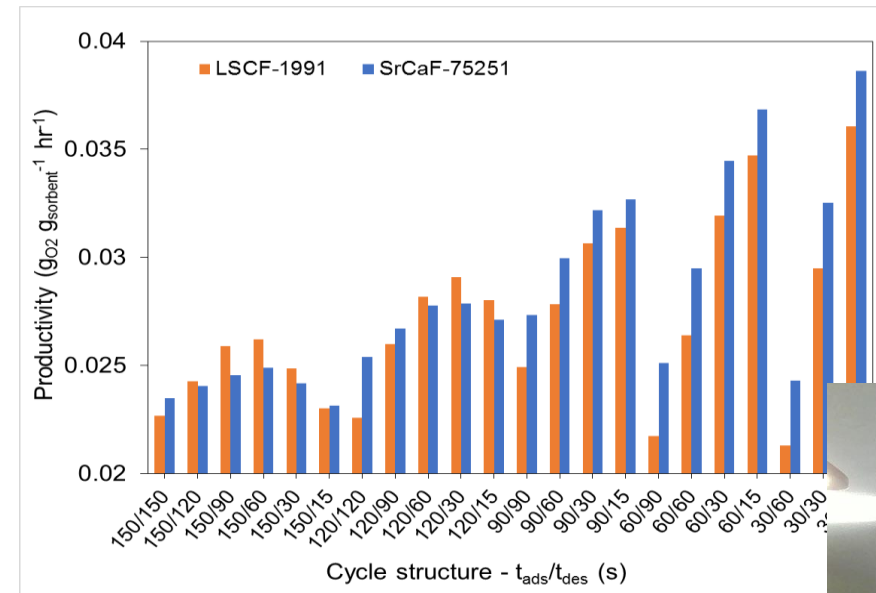
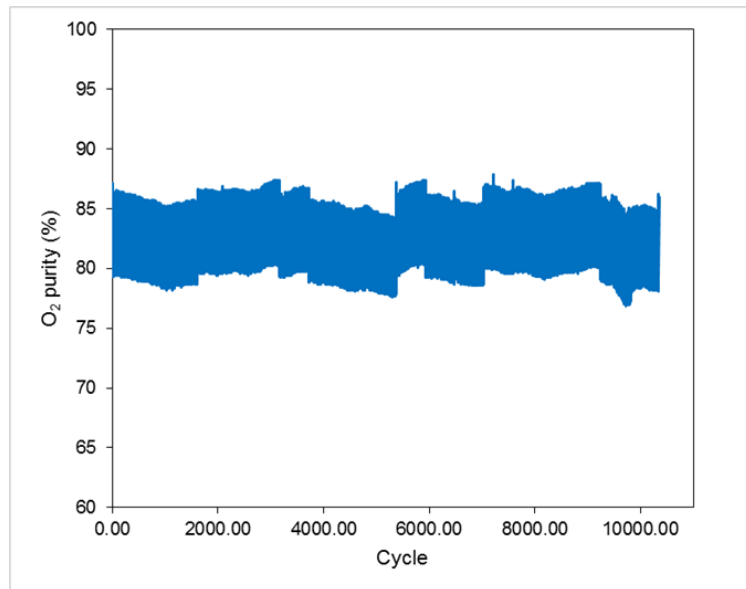
(Larger rates suggest use



Perovskite Characterization

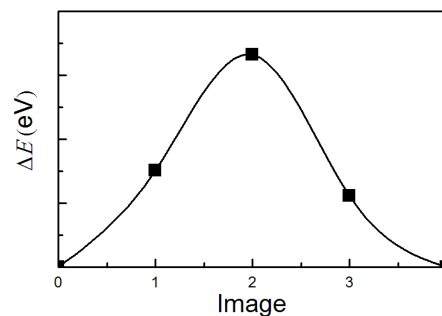
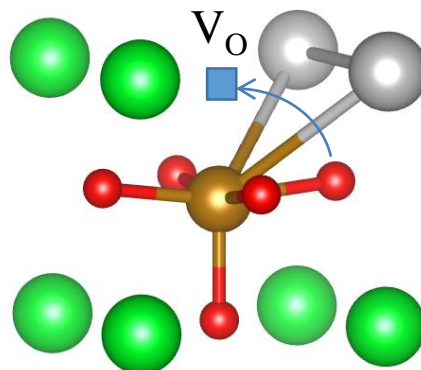
Stability Testing and Comparison to Known Materials

- NETL Perovskite samples were tested in collaboration with ThermoSolv
- NETL sample demonstrated stability over $>10,000$ cycles
- NETL Perovskite outperformed an LSCF sample in multiple cycle structures

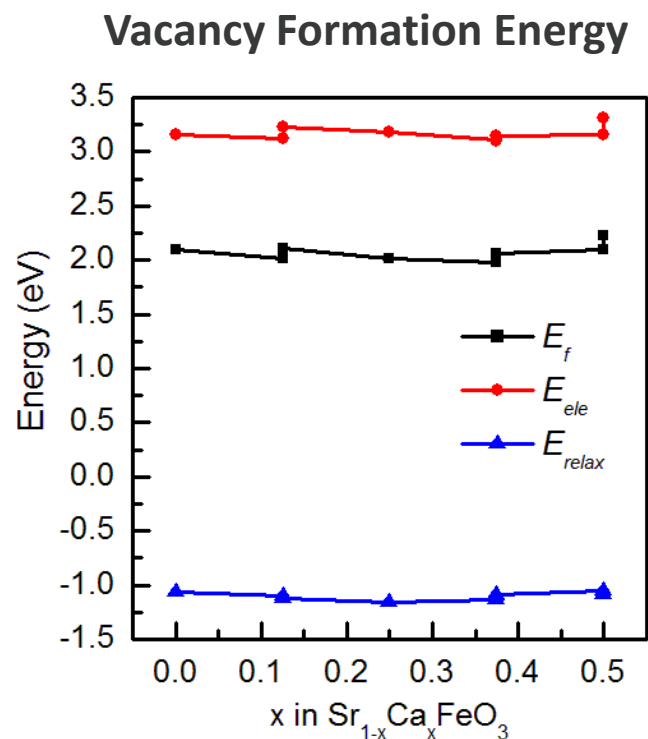


Perovskite Modelling

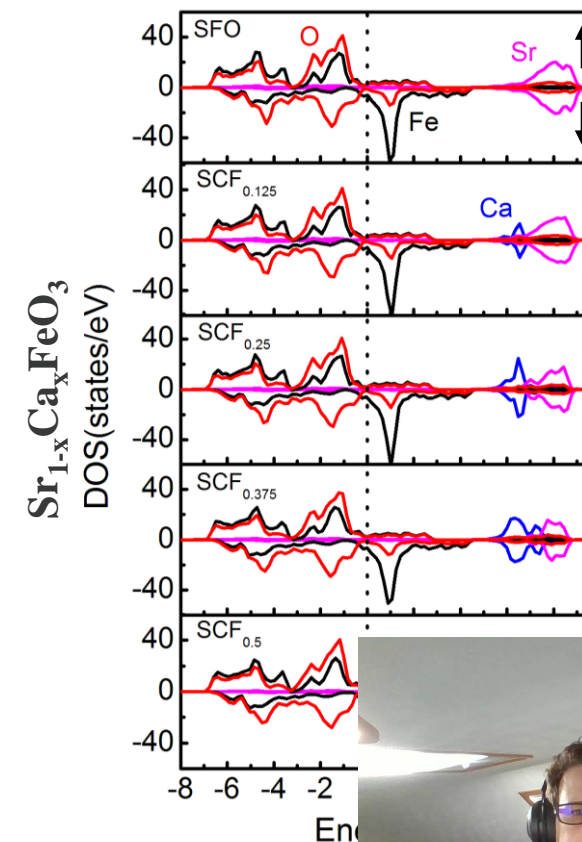
Atomistic Modelling



Oxygen Diffusion

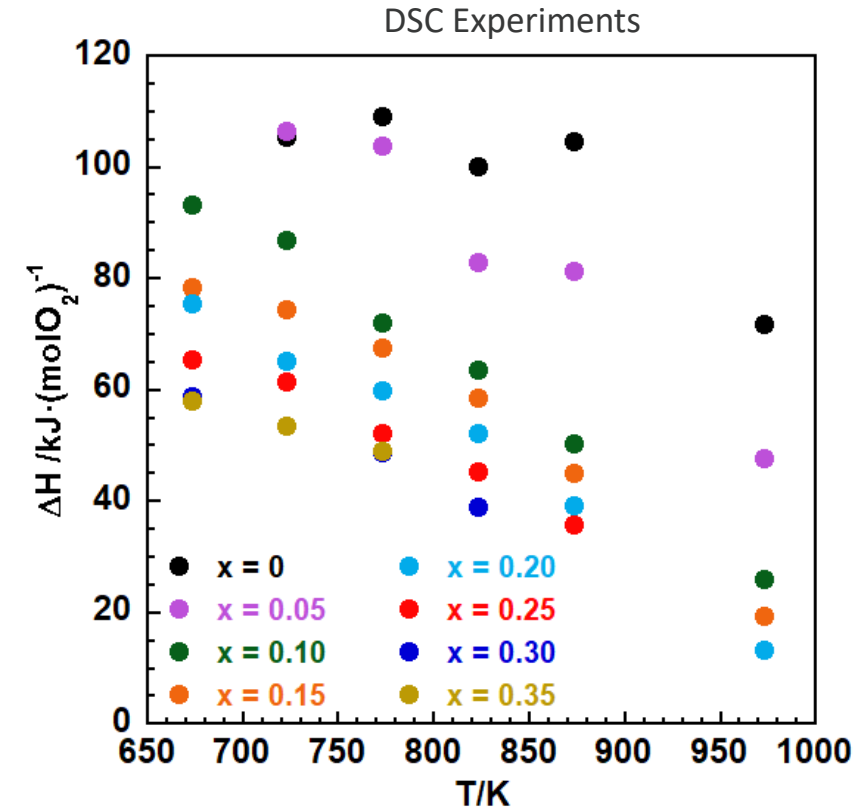
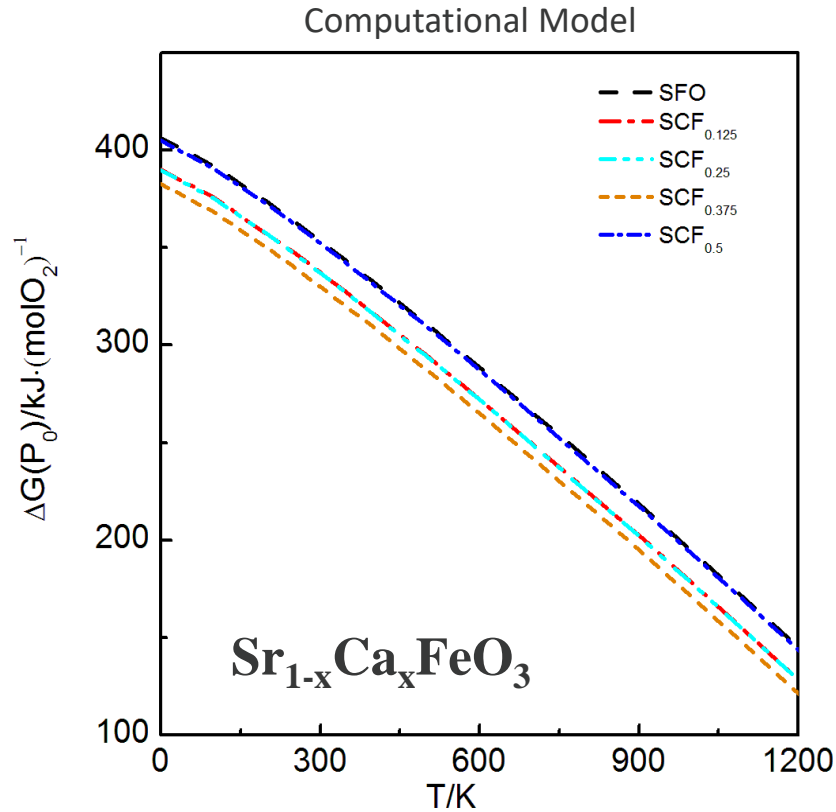


Electronic Density of States



Perovskite Modelling

Ellingham Diagram Calculation

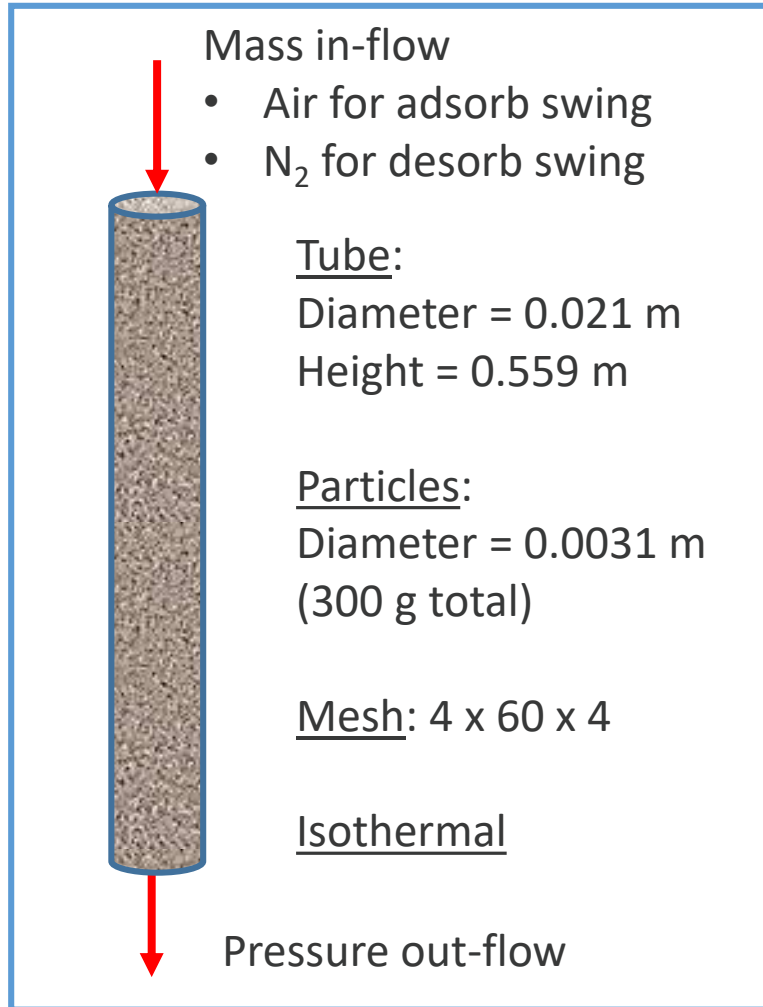


- Differential Scanning Calorimetry used to determine enthalpy of oxidation/reduction for each sample at each temperature from cycling experiments
- Decreasing enthalpy as both calcium content and temperature increase
- Agreement between computational models and DSC experiments

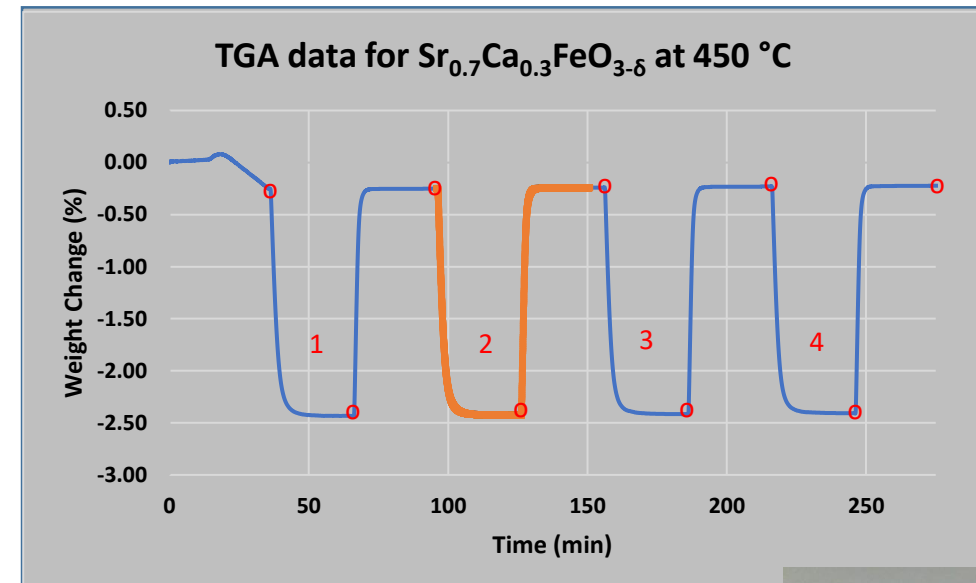


Perovskite Modeling

MFiX-DEM Verification of TGA Data

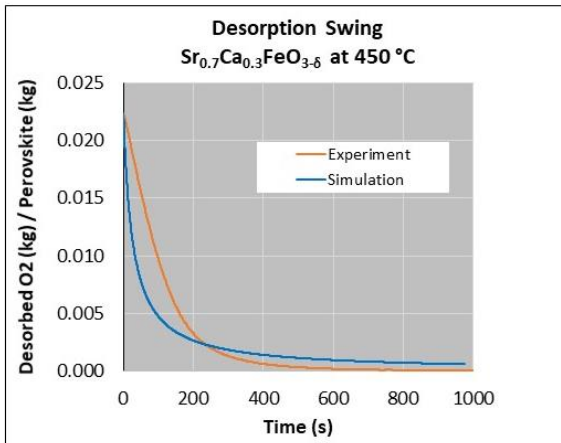
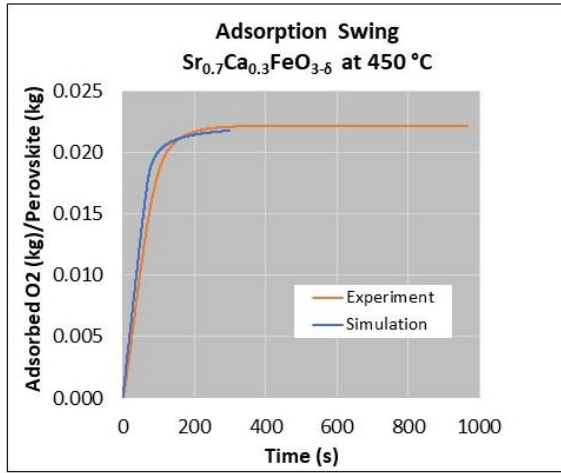


For each case, the 2nd TGA cycle was used to calculate kinetic constants.



Current and Future Work

MFiX Validation and Reactor Design

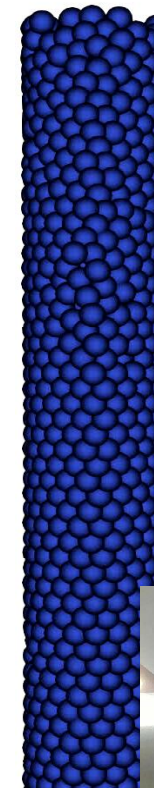
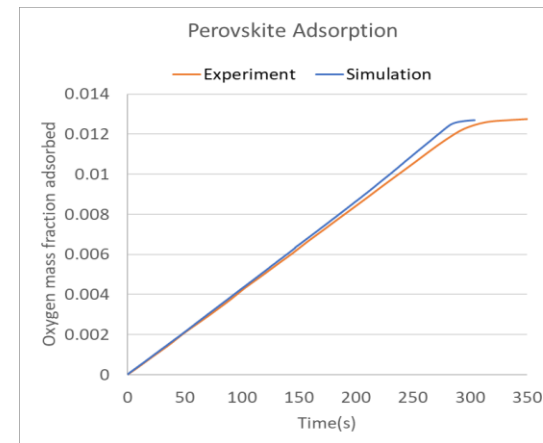


Validated TGA data
will contribute to the

final MFiX CFD
Reactor Design

CFD Model Demonstration for 300s O₂ absorption sweep

- 22mm x 559mm tube
- Ba_{1-x}Sr_xCo_{0.8}Fe_{0.2}O_{3-delta} data from He (2009)



Mass fraction
O₂ absorbed
at tube inlet
for first 30s

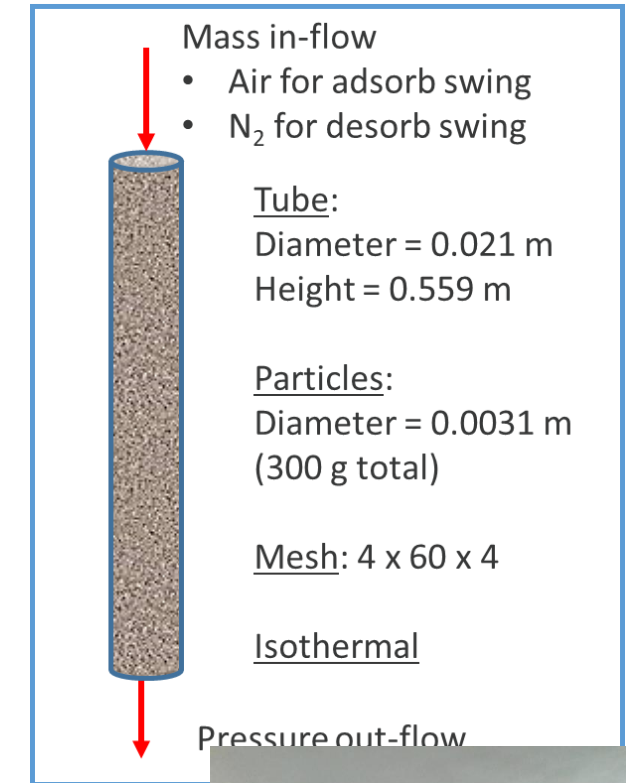
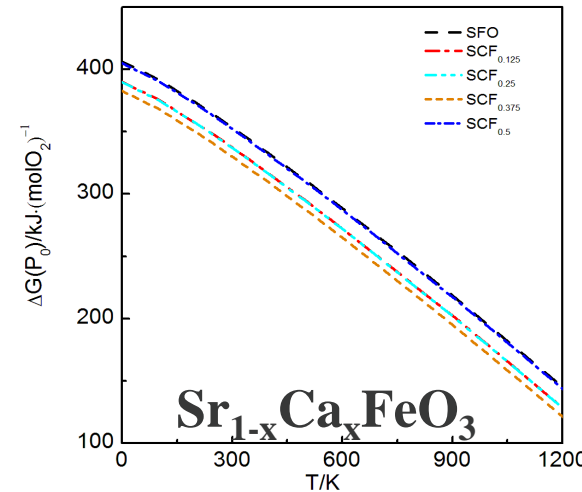
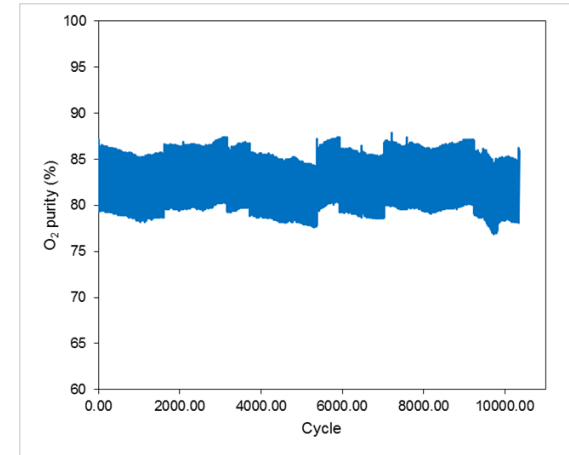
1.3e-02
0.01

For each temperature and perovskite composition, a numerical matching of TGA data is necessary.



Conclusions

- Synthesized more than 24 perovskite materials
- Achieved more than 2.4 wt % O₂ capacity
- Achieved control of desorption temperature
- Sr_{1-x}Ca_xFeO_{3-d} found to outperform LSCF
- Sr_{1-x}Ca_xFeO_{3-d} found to be stable over >10,000 cycles
- Experimentally validated Ellingham Diagrams
- Initiated CFD design and model validation



Acknowledgements



- **Experimental**

- Eric Popczun
- Sittichai Natesakhawat
- Christopher Marin
- Thuy-Duong Nguyen-Phan
- Douglas Kauffman
- Yunyun Zhou

- **Computational**

- Yuhua Duan
- Ting Jia
- Dominic Alfonso
- De Nyago Tafen
- William Rogers
- Mehrdad Shahnam
- MaryAnn Clarke
- Deepthi Chandramouli

- **Collaborators**

- Wenqian Xu
- Andrey Yakovenko
- Chrysanthos Gounaris
- Christopher Hanselman
- Anthony Richard



- **DISCLAIMER**

- This project was funded by the Department of Energy, National Energy Technology Laboratory, an agency of the United States Government, through a support contract with AECOM. Neither the United States Government nor any agency thereof, nor any of their employees, nor AECOM, nor any of their employees, makes any warranty, expressed or implied, or assumes any legal liability or responsibility for the accuracy, completeness, or usefulness of any information, apparatus, or process disclosed, or represents that its use would not infringe upon or otherwise violate any patent rights. Reference herein to any specific commercial product, process, or service by name, trademark, manufacturer, or otherwise, does not necessarily constitute an endorsement, recommendation, or favoring by the United States Government or any agency thereof. The views and opinions of authors expressed herein do not necessarily state or reflect those of the United States Government or any agency thereof.



Questions?



Solutions for Today | Options for Tomorrow

